NASA TECHNICAL NOTE

NASA TN D-2930

NASA TN D-2930

A METHOD OF DETERMINING MODAL DATA OF A NONUNIFORM BEAM WITH EFFECTS OF SHEAR DEFORMATION AND ROTARY INERTIA

by Vernon L. Alley, Jr., Robert J. Guillotte, and Lessie D. Hunter

Langley Research Center
Langley Station, Hampton, Va.

NATIONAL AERONAUTICS AND SPACE ADMINISTRATION • WASHINGTON, D. C. • SEPTEMBER 1965

NASA TN D-2930

A METHOD OF DETERMINING MODAL DATA OF A NONUNIFORM BEAM WITH EFFECTS OF SHEAR DEFORMATION AND ROTARY INERTIA

By Vernon L. Alley, Jr., Robert J. Guillotte,
and Lessie D. Hunter

Langley Research Center
Langley Station, Hampton, Va.

NATIONAL AERONAUTICS AND SPACE ADMINISTRATION

For sale by the Clearinghouse for Federal Scientific and Technical Information
Springfield, Virginia 22151 – Price $2.00

A METHOD OF DETERMINING MODAL DATA OF A NONUNIFORM BEAM WITH EFFECTS OF SHEAR DEFORMATION AND ROTARY INERTIA

By Vernon L. Alley, Jr., Robert J. Guillotte,
and Lessie D. Hunter
Langley Research Center

SUMMARY

A recurrence solution including the secondary effects of rotary inertia and shear deformation on discontinuous nonuniform beamlike structures is presented for obtaining highly descriptive free-free natural mode data. Results of other studies are included to ascertain the significance of the secondary influences on the classical uniform beam. Numerical results are also included for the application of the method to a first-stage and fourth-stage configuration of a typical space research launch vehicle. The numerical results indicate that shear deformation is generally the prime contributor of the secondary effects on typical launch vehicle configurations; the major influences of the secondary effects are seen in reductions in natural frequencies and in changes to the mode slopes, mode moments, and mode shears.

INTRODUCTION

Natural vibration characteristics are frequently required for systems that can be appropriately represented as free-free beamlike structures. Such structures are consistently encountered in the array of stages that comprise the typical launch vehicle for space research.

An assessment of the natural vibration characteristics normally will include the calculations of the fundamental frequencies of oscillation along with a number of overtones. The deflected curves associated with each characteristic frequency, known as either mode shapes, characteristic functions, or eigenfunctions, are also desired data. In addition, the slopes, moments, and sometimes the shears associated with the mode shape are provided. Special definite integrals also are frequently computed, for example, the generalized or effective mass of a mode.

These data have a variety of uses. Their most familiar use is in providing knowledge of natural frequencies for designing in order to avoid states of resonant vibrations. This application is particularly important in designing or qualifying the spin program for unguided launch vehicles. (Trajectory dispersion control is frequently accomplished by spinning a vehicle about its longitudinal axis.) High dynamic stresses and even structural failures might

result if the roll frequency is near or coincident for an appreciable time to one of the natural frequencies of the system.

In addition, the vibration response levels of a vehicle will generally be high near the frequencies of the natural vibrations of the basic structure. Knowledge of the probable distribution of the disturbance spectrum can provide information for appropriate shock mounting of delicate payloads and can lead to a proper choice of the dynamic characteristics of instrumentation.

Furthermore, calculated mode shapes and frequencies can be useful in interpreting measured vibration data. For example, moment and shear data associated with calculated modal responses are frequently used for rapid assessment of the load significance of recorded flight data.

Probably the greatest value of modal data is realized in series solutions of the differential equations of motion of the system for which they have been generated. The well-known orthogonality properties of mode shapes, the fact that the modes satisfy the appropriate boundary conditions for their particular constraints, and the fact that the usual response of a beam system is adequately described by superposition of a few modes make them ideal functions for such applications, widely known as modal form solutions.

The modal form series solution is particularly adaptable to formulating techniques for yielding gust, wind loads, ignition and separation responses, and other transient loads. The modal form approach has also proven popular for developing the characteristic equation of structures coupled with closed-loop autopilot systems. Such analyses permit investigations of the stability boundaries of such systems and lead to proper gain levels and filter characteristics to yield stable performances.

Such valuable applications of modal data have stimulated analysts to develop a variety of analytical techniques to achieve increased accuracy and scope of output with a minimization of input effort. Well-known and fundamental considerations of beam vibration are presented by Den Hartog in reference 1. The classical techniques of Rayleigh and Stodola are two of the methods discussed in detail by Hartog. In reference 2, Scanlan and Rosenbaum describe the classical procedure attributed to Rayleigh and Ritz along with the Myklestad method. They proceed to meticulously outline a step-by-step matrix method employing influence coefficients. This latter procedure has been formulated into a rigorous matrix solution and is presented by Alley and Gerringer in reference 3. Houbolt and Anderson have organized the method of Stodola and presented other useful related material in reference 4. An interesting integral series solution technique that is also an effective solution to the nonuniform beam vibration problem is presented by Spector in reference 5. These references are but a few of the publicized methods relating to natural vibrations of nonuniform beams.

When the analyst is confronted with a particular assignment for computing modal data, the choice of the most suitable method should be made in view of the objectives of the assignment and the virtues and limitations that characterize the methods. Energy methods following the concepts of Rayleigh or the

Rayleigh-Ritz approach generally yield adequate results on frequencies but possess weaknesses in the exactness and descriptiveness of the mode shapes and their derivatives. The classical Myklestad method as well as the matrix method of reference 3 treat the system as a number of lumped point masses coupled with massless springs. These discrete mass models also yield adequate frequency data but suffer a loss in descriptiveness of the other modal data, particularly in the shear curves associated with the modes. The Stodola process, or one similar, requires iteration to converge on both frequency and mode shape. Whereas the frequency is readily obtained to a desired accuracy, the mode shape is not so readily made everywhere convergent to a prescribed accuracy. In addition, the procedure requires sweeping techniques to obtain modes of higher frequencies than the fundamental. This operation frequently presents practical problems due to degeneration in numerical accuracy. The integral series method, although capable of yielding both the fundamental and higher modes, presents a formidable computing problem, the maintenance of sufficient accuracy in performing numerically the required multi-integrations. In the original or classical form, all of the aforementioned methods omit the secondary influences of rotary inertia and shear deformation. Many extensions to the classical forms have been made throughout industry and government, yet few satisfactory methods incorporating the secondary influences have been adequately described in generally available literature. Shear deformation introduces an additional source of deflection to the customary flexural deformation considered in elementary beam theory. Cross-section rotary inertia provides additional dynamic loading to the system due to the rotational acceleration of the cross section of the beam. In most slender beams the shear and rotary inertia contributions to loading and deflection are small in comparison with those resulting directly from bending. In multistage launch vehicles of conventional fabrication the shear deformation is secondary to bending and the structure is generally so slender that rotary inertia may also be ignored.

However, the use of fiber-glass stages has given unexpected emphasis to the importance of shear. The low ratio of shear modulus to the flexural modulus of elasticity of fiber glass increases the relative contribution of shear deformation to bending and thus produces significant shear effects in geometries that otherwise could be investigated adequately without considering secondary effects.

In addition, when computing the modal data of beam systems with low length-to-diameter ratios such as characterized by the upper stages of conventional multistage launch vehicles, the inclusion of both shear deformation and rotary inertia has been found to be important to data accuracies.

This paper presents another technique for computing modal data on nonuniform beams. The method has proven very satisfactory for accurately describing not only the mode shape, but its slope, mode moments, and mode shears. The method is inherently applicable to structures exhibiting numerous discontinuities in their mass and stiffness properties and requires no discreting to an analogous lumped mass system. The differential equations of motion of the beam system are dealt with directly. Modes need not be computed consecutively as is required by a number of other methods. The technique has been employed successfully in obtaining accurate modal data up to the tenth mode on complex

structures. Furthermore, the formulation accurately incorporates the secondary influences of rotary inertia and shear deformation.

The organization of the problem in the matrix form that follows has proven to be highly practical in obtaining numerical solutions on a high-speed digital computer. Also, the numerical integration technique that is an integral part of the method has been found to be highly stable and accurate.

The detailed mathematical developments of the method are presented with information pertinent to practical numerical solutions utilizing the digital computer. Some data are supplied for assessing the probable importance of the secondary influences. An example of the application of the method to a typical four-stage launch vehicle is submitted with a study of the importance of secondary influences on the upper stage.

SYMBOLS

A	cross-sectional area in shear, $in.^2$
"A"	solution for superposition method
A_1	value of ψ' at x_l due to a unit value of ψ at x_a, $in.^{-1}$
A_2	value of V at x_l due to a unit value of ψ at x_a, lb/rad
a	coefficient (eqs. (30)), $m_{n+1}\omega^2$, $lb\text{-}rad^2/in.^2$
"B"	solution for superposition method
B_1	value of ψ' at x_l due to a unit value of ζ at x_a, $rad/in.^2$
B_2	value of V at x_l due to a unit value of ζ at x_a, lb/in.
b	coefficient (eqs. (30)), $Z_{n+1}\omega^2$, $lb\text{-}rad^2/in.^2$
C_1	value of ζ at x_l due to a unit value of ψ at x_a, in./rad
C_2	value of ψ at x_l due to a unit value of ψ at x_a, unitless
D	maximum diameter of beam, in.; also used as determinant (eq. (32))
D_1	value of ζ at x_l due to a unit value of ζ at x_a, unitless
D_2	value of ψ at x_l due to a unit value of ζ at x_a, rad/in.

d	shear deformation coefficient (eqs. (30)), $\frac{1}{KAG}$, lb^{-1}
E	modulus of elasticity in bending, $lb/in.^2$
e	flexibility coefficient (eqs. (30)), $\frac{1}{EI}$, $lb^{-1}\text{-}in.^{-2}$
$f(\omega)$	frequency equation (eq. (37))
G	modulus of shear, $lb/in.^2$
I	area moment of inertia for a given cross section, $in.^4$
K	coefficient for cross section in shear
k_r	effective spring constant of the rth mode; lb/in. when mode shapes are considered dimensionless
k	half increment (eqs. (30)), $\Delta x/2$, in.
L	overall length of beam, in.
M	mode moment due to bending, in-lb
m	mass per inch of length, $lb\text{-}sec^2/in.^2$
m_r	effective mass of the rth mode; $lb\text{-}sec^2$/in. when mode shapes are considered dimensionless
P_{n+1}	matrix in recurrence solution of equation (27)
p	point in derivation
t	time, sec
V	mode shear due to bending, lb/in.
X	column matrix of variables (see eq. (10))
x	coordinate along length of vehicle, in.
x_a	value of x at extreme left end of beam (lower boundary), in.
x_l	value of x at extreme right end of beam (upper boundary), in.
Δx	increment in recurrence solution, $x_{n+1} - x_n$, in.
Z	rotary inertia, $lb\text{-}sec^2$

β	matrix (see eq. (10))
δ_1	matrix (see eq. (19))
δ_2	matrix (see eq. (20))
ζ	deflection, in.
Λ	matrix (see eq. (21))
λ	approximation of second derivative of variable (see eqs. (12) to (15) and (21))
ψ	cross-sectional rotation due to bending, rad
ω	circular frequency, rad/sec
$\Delta\omega$	increment of ω in trial solutions

Subscripts:

A	"A" solution
a	lower boundary
B	"B" solution
l	upper boundary
n	body station
r	mode

Matrix notations:

$\{\ \}$	column matrix
$[\ ]$	square or rectangular matrix
$[\ ]^{-1}$	inverse matrix
$\lfloor 1 \rceil$	unit matrix

Primed symbols denote differentiation with respect to x.

DERIVATION OF THE METHOD

A derivation is presented for the differential equation of an oscillating beam structure expressed as a set of four first-order differential equations. A recurrence formula is established which relates the system variables (mode shapes, mode slopes, mode moments, and shears, and their derivatives) at one station of the beam to those at an adjoining station. Boundary equations are established for the free-free system and a characteristic equation is obtained for computing the critical frequencies of the system. Treatment of discontinuities is considered in detail, and the orthogonality and equilibrium relations are established.

Equations of Motion

A sketch is presented which shows the equations of motion.

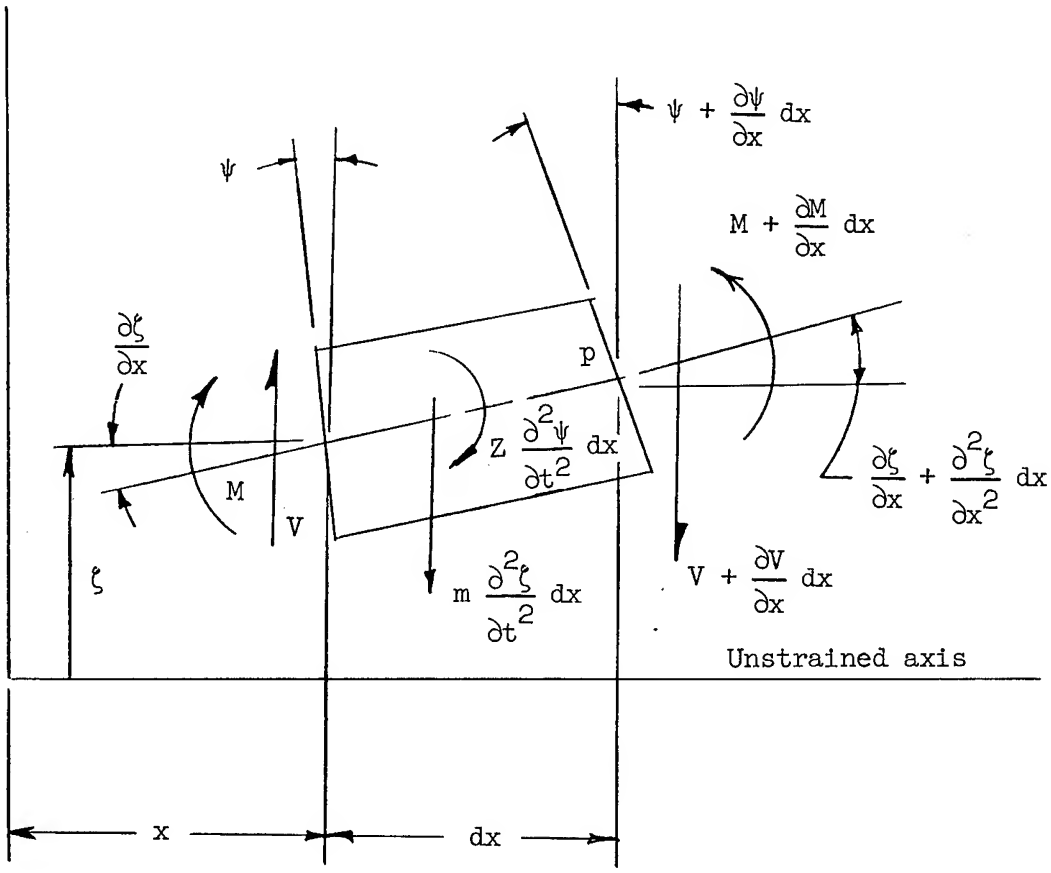

Consider the differential element of a beam of dx length in the sketch, then the summation of the vertical forces on the element will yield

$$m \frac{\partial^2 \zeta}{\partial t^2} dx + \frac{\partial V}{\partial x} dx = 0 \tag{1}$$

Summing moments about p and dropping second-order terms gives

$$V\, dx + Z \frac{\partial^2 \psi}{\partial t^2} dx - \frac{\partial M}{\partial x} dx = 0 \tag{2}$$

From elementary beam theory, it is known that

$$V = -KAG\left(\frac{\partial \zeta}{\partial x} - \psi\right) \tag{3}$$

$$M = EI \frac{\partial \psi}{\partial x} \tag{4}$$

where ψ is the cross-section rotation due to bending which differs from $\partial\zeta/\partial x$ because of shear deformation.

Also, if interest is confined to the undamped rth natural mode, solutions of ζ, ψ, V, and M are assumed to have the form

$$\left.\begin{aligned} \zeta(x,t) &= \zeta_r(x)e^{i\omega_r t} \\ \psi(x,t) &= \psi_r(x)e^{i\omega_r t} \\ V(x,t) &= V_r(x)e^{i\omega_r t} \\ M(x,t) &= M_r(x)e^{i\omega_r t} \end{aligned}\right\} \tag{5}$$

where ω_r is the angular frequency of undamped harmonic motion in the rth mode.

It should also be noted that KAG and EI are functions of x only; therefore

$$\frac{\partial(KAG)}{\partial x} = \frac{d(KAG)}{dx}$$

$$\frac{\partial(EI)}{\partial x} = \frac{d(EI)}{dx}$$

Substituting equations (5) in equations (1) to (4) and performing the indicated differentiations gives the basic form of the differential equations for the natural vibration of a beam, consideration being given to flexure, shear deformation, and rotary inertia. Henceforth the subscripts will be dropped for purposes of clarity, and the equations will appear as

$$-m\omega^2\zeta + \frac{dV}{dx} = 0 \tag{6}$$

$$V - Z\omega^2\psi - \frac{dM}{dx} = 0 \tag{7}$$

$$\frac{d\zeta}{dx} + \frac{V}{KAG} - \psi = 0 \tag{8}$$

$$\frac{M}{EI} - \frac{d\psi}{dx} = 0 \tag{9}$$

Expressed in matrix notation, equations (6) to (9) appear as

$$\begin{bmatrix} 0 & -m\omega^2 & 0 & 0 & 1 & 0 & 0 & 0 \\ 0 & 0 & 0 & -Z\omega^2 & 0 & 1 & -1 & 0 \\ 1 & 0 & 0 & -1 & 0 & \frac{1}{KAG} & 0 & 0 \\ 0 & 0 & -1 & 0 & 0 & 0 & 0 & \frac{1}{EI} \end{bmatrix} \begin{Bmatrix} \zeta' \\ \zeta \\ \psi' \\ \psi \\ V' \\ V \\ M' \\ M \end{Bmatrix} = 0 \tag{10}$$

where the primes denote differentiation with respect to x.

If the 4×8 matrix in equation (10) is denoted as β, and the 8×1 column matrix of unknowns as X, then equation (10) may be written as

$$[\beta]\{X\} = 0 \tag{11}$$

The matrix equation (eq. (11)) constitutes the equations of motion of the system.

Recurrence Solution

The following relationships are introduced and are based on the assumption that the first derivatives of the system variables are linear over the small increment x_n to x_{n+1}. Let $(x_{n+1} - x_n) = \Delta x$.

$$\left.\begin{aligned} \frac{d\zeta_{n+1}}{dx} &= \frac{d\zeta_n}{dx} + \Delta x \lambda_n(\zeta) \\ \zeta_{n+1} &= \frac{d\zeta_n}{dx}\Delta x + \zeta_n + \frac{\Delta x^2}{2}\lambda_n(\zeta) \end{aligned}\right\} \tag{12}$$

$$\left.\begin{aligned} \frac{d\psi_{n+1}}{dx} &= \frac{d\psi_n}{dx} + \Delta x \lambda_n(\psi) \\ \psi_{n+1} &= \frac{d\psi_n}{dx}\Delta x + \psi_n + \frac{\Delta x^2}{2}\lambda_n(\psi) \end{aligned}\right\} \tag{13}$$

$$\left.\begin{aligned} \frac{dV_{n+1}}{dx} &= \frac{dV_n}{dx} + \Delta x \lambda_n(V) \\ V_{n+1} &= \frac{dV_n}{dx}\Delta x + V_n + \frac{\Delta x^2}{2}\lambda_n(V) \end{aligned}\right\} \tag{14}$$

$$\left.\begin{aligned} \frac{dM_{n+1}}{dx} &= \frac{dM_n}{dx} + \Delta x \lambda_n(M) \\ M_{n+1} &= \frac{dM_n}{dx}\Delta x + M_n + \frac{\Delta x^2}{2}\lambda_n(M) \end{aligned}\right\} \tag{15}$$

At this point $\lambda_n(\zeta)$, $\lambda_n(\psi)$, et cetera, are to be regarded as undetermined.

Equations (12) to (15) may be written in matrix notation:

$$\begin{Bmatrix} \zeta'_{n+1} \\ \zeta_{n+1} \\ \psi'_{n+1} \\ \psi_{n+1} \\ V'_{n+1} \\ V_{n+1} \\ M'_{n+1} \\ M_{n+1} \end{Bmatrix} = \begin{bmatrix} 1 & 0 & 0 & 0 & 0 & 0 & 0 & 0 \\ \Delta x & 1 & 0 & 0 & 0 & 0 & 0 & 0 \\ 0 & 0 & 1 & 0 & 0 & 0 & 0 & 0 \\ 0 & 0 & \Delta x & 1 & 0 & 0 & 0 & 0 \\ 0 & 0 & 0 & 0 & 1 & 0 & 0 & 0 \\ 0 & 0 & 0 & 0 & \Delta x & 1 & 0 & 0 \\ 0 & 0 & 0 & 0 & 0 & 0 & 1 & 0 \\ 0 & 0 & 0 & 0 & 0 & 0 & \Delta x & 1 \end{bmatrix} \begin{Bmatrix} \zeta'_n \\ \zeta_n \\ \psi'_n \\ \psi_n \\ V'_n \\ V_n \\ M'_n \\ M_n \end{Bmatrix} + \begin{bmatrix} \Delta x & 0 & 0 & 0 \\ \frac{\Delta x^2}{2} & 0 & 0 & 0 \\ 0 & \Delta x & 0 & 0 \\ 0 & \frac{\Delta x^2}{2} & 0 & 0 \\ 0 & 0 & \Delta x & 0 \\ 0 & 0 & \frac{\Delta x^2}{2} & 0 \\ 0 & 0 & 0 & \Delta x \\ 0 & 0 & 0 & \frac{\Delta x^2}{2} \end{bmatrix} \begin{Bmatrix} \lambda_n(\zeta) \\ \lambda_n(\psi) \\ \lambda_n(V) \\ \lambda_n(M) \end{Bmatrix} \tag{16}$$

Let

$$\{X_{n+1}\} = \begin{Bmatrix} \zeta'_{n+1} \\ \zeta_{n+1} \\ \psi'_{n+1} \\ \psi_{n+1} \\ V'_{n+1} \\ V_{n+1} \\ M'_{n+1} \\ M_{n+1} \end{Bmatrix} \tag{17}$$

$$\left[\delta_1\right] = \begin{bmatrix} 1 & 0 & 0 & 0 & 0 & 0 & 0 & 0 \\ \Delta x & 1 & 0 & 0 & 0 & 0 & 0 & 0 \\ 0 & 0 & 1 & 0 & 0 & 0 & 0 & 0 \\ 0 & 0 & \Delta x & 1 & 0 & 0 & 0 & 0 \\ 0 & 0 & 0 & 0 & 1 & 0 & 0 & 0 \\ 0 & 0 & 0 & 0 & \Delta x & 1 & 0 & 0 \\ 0 & 0 & 0 & 0 & 0 & 0 & 1 & 0 \\ 0 & 0 & 0 & 0 & 0 & 0 & \Delta x & 1 \end{bmatrix} \tag{18}$$

$$\left\{X_n\right\} = \begin{Bmatrix} \zeta_n' \\ \zeta_n \\ \psi_n' \\ \psi_n \\ V_n' \\ V_n \\ M_n' \\ M_n \end{Bmatrix} \tag{19}$$

$$\left[\delta_2\right] = \begin{bmatrix} 1 & 0 & 0 & 0 \\ \frac{\Delta x}{2} & 0 & 0 & 0 \\ 0 & 1 & 0 & 0 \\ 0 & \frac{\Delta x}{2} & 0 & 0 \\ 0 & 0 & 1 & 0 \\ 0 & 0 & \frac{\Delta x}{2} & 0 \\ 0 & 0 & 0 & 1 \\ 0 & 0 & 0 & \frac{\Delta x}{2} \end{bmatrix} \tag{20}$$

and

$$\left\{\Lambda_n\right\} = \begin{Bmatrix} \lambda_n(\zeta) \\ \lambda_n(\psi) \\ \lambda_n(V) \\ \lambda_n(M) \end{Bmatrix} \tag{21}$$

Then, from the relationships (17) to (21), equation (16) becomes

$$\left\{X_{n+1}\right\} = \left[\delta_1\right]\left\{X_n\right\} + \Delta x\left[\delta_2\right]\left\{\Lambda_n\right\} \tag{22}$$

The system variables must now satisfy the equations of motion at any specified station. That is, when $x = x_{n+1}$,

$$\left[\beta_{n+1}\right]\left\{X_{n+1}\right\} = 0 \tag{23}$$

by virtue of the constraint imposed through the following determination of the Λ matrix. Substituting equation (22) in equation (23) gives

$$\left[\beta_{n+1}\right]\left[\left[\delta_1\right]\left\{X_n\right\} + \Delta x\left[\delta_2\right]\left\{\Lambda_n\right\}\right] = 0 \tag{24}$$

Solving equation (24) for Λ_n yields

$$\left\{\Lambda_n\right\} = -\frac{1}{\Delta x}\left[\left[\beta_{n+1}\right]\left[\delta_2\right]\right]^{-1}\left[\beta_{n+1}\right]\left[\delta_1\right]\left\{X_n\right\} \tag{25}$$

Thus, the variables $\lambda(\zeta)$, $\lambda(\psi)$, et cetera which were undetermined in equations (12) to (15) are defined by requiring satisfaction of equation (23). Substituting equation (25) into equation (22) gives the recurrence formula for the functions ζ, ψ, V, and M:

$$\left\{X_{n+1}\right\} = \left[\left[1\right] - \left[\delta_2\right]\left[\left[\beta_{n+1}\right]\left[\delta_2\right]\right]^{-1}\left[\beta_{n+1}\right]\right]\left[\delta_1\right]\left\{X_n\right\} \tag{26}$$

It is expedient to perform the matrix manipulations to express equation (26) in the form

$$\left\{X_{n+1}\right\} = \left[P_{n+1}\right]\left\{X_n\right\} \tag{27}$$

where

$$\left[P_{n+1}\right] = \left[\left[1\right] - \left[\delta_2\right]\left[\left[\beta_{n+1}\right]\left[\delta_2\right]\right]^{-1}\left[\beta_{n+1}\right]\right]\left[\delta_1\right] \tag{28}$$

From equations (10), (11), and (20) it can be seen that

$$\left[\beta_{n+1}\right]\left[\delta_2\right] = \begin{bmatrix} -m_{n+1}\omega^2 \frac{\Delta x}{2} & 0 & 1 & 0 \\ 0 & -Z_{n+1}\omega^2 \frac{\Delta x}{2} & \frac{\Delta x}{2} & -1 \\ 1 & -\frac{\Delta x}{2} & \frac{1}{KAG_{n+1}} \frac{\Delta x}{2} & 0 \\ 0 & -1 & 0 & \frac{1}{EI_{n+1}} \frac{\Delta x}{2} \end{bmatrix} \tag{29}$$

For convenience, let

$$\left.\begin{aligned} a &= m_{n+1}\omega^2 \\ b &= Z_{n+1}\omega^2 \\ d &= KAG_{n+1}^{-1} \\ e &= EI_{n+1}^{-1} \\ k &= \frac{\Delta x}{2} \end{aligned}\right\} \tag{30}$$

Then, equation (29) may be expressed as

$$\left[\beta_{n+1}\right]\left[\delta_2\right] = \begin{bmatrix} -ak & 0 & 1 & 0 \\ 0 & -bk & k & -1 \\ 1 & -k & dk & 0 \\ 0 & -1 & 0 & ek \end{bmatrix} \tag{31}$$

The determinant D of this matrix is given by the formula

$$D = -aek^4 + \left(1 + bek^2\right)\left(1 + adk^2\right) \tag{32}$$

By utilizing equations (10), (11), (19), (20), and (30) and by performing the matrix operations indicated in equation (26), the elements of the matrix P_{n+1}, which appears in equation (27), may be reduced to the explicit algebraic expressions given in equation (33). The elements are functions only of the structural properties at x_n and x_{n+1}, of the interval length Δx, and of the unknown-frequency ω. Equations (32) and (33) provide the working relationships for practical use of the recurrence formula given by equation (27).

$$\left[P_{n+1}\right] = \frac{1}{D}\begin{bmatrix} ak^2\left[ek^2(1-bd)-d\right] & ak\left[ek^2(1-bd)-d\right] & k & 1 & \left[ek^2(1-bd)-d\right]k & \left[ek^2(1-bd)-d\right] & ek^2 & ek \\ k\left(1+bek^2\right) & 1+bek^2 & k^2 & k & \left[ek^2(1-bd)-d\right]k^2 & \left[ek^2(1-bd)-d\right]k & ek^3 & ek^2 \\ aek^3 & aek^2 & ek^2\left[ak^2(1-bd)-b\right] & ek\left[ak^2(1-bd)-b\right] & ek^2 & ek & ek\left(1+adk^2\right) & e\left(1+adk^2\right) \\ aek^4 & aek^3 & k\left(1+adk^2\right) & 1+adk^2 & ek^3 & ek^2 & ek^2\left(1+adk^2\right) & ek\left(1+adk^2\right) \\ a\left(1+bek^2\right)k & a\left(1+bek^2\right) & ak^2 & ak & ak^2\left[ek^2(1-bd)-d\right] & ak\left[ek^2(1-bd)-d\right] & aek^3 & aek^2 \\ a\left(1+bek^2\right)k^2 & a\left(1+bek^2\right)k & ak^3 & ak^2 & k\left(1+bek^2\right) & 1+bek^2 & aek^4 & aek^3 \\ ak^2 & ak & \left[ak^2(1-bd)-b\right]k & \left[ak^2(1-bd)-b\right] & k & 1 & ek^2\left[ak^2(1-bd)-b\right] & ek\left[ak^2(1-bd)-b\right] \\ ak^3 & ak^2 & \left[ak^2(1-bd)-b\right]k^2 & \left[ak^2(1-bd)-b\right]k & k^2 & k & k\left(1+adk^2\right) & 1+adk^2 \end{bmatrix} \tag{33}$$

Boundary Conditions

In the work that follows, the solution will be restricted to considerations of the free-free vibration behavior. This mode of behavior is appropriate to the in-flight characteristics of launch vehicles. Henceforth, the subscripts a and l indicate that the associated quantity is evaluated at the lower boundary $x = x_a$ or at the upper boundary $x = x_l$, respectively. The boundary conditions at both ends of a free-free beam require that

Condition (a):

$$V_a = V_l = 0$$

Condition (b):

$$M_a = M_l = 0$$

Substituting condition (a) in equation (8) shows that

Condition (c):

$$\zeta_a' = \psi_a$$

Condition (d):

$$\zeta_l' = \psi_l$$

Substituting condition (a) in equation (7) gives

Condition (e):

$$M_a' = -Z_a\omega^2\psi_a$$

Condition (f):

$$M_l' = -Z_l\omega^2\psi_l$$

Substituting condition (b) in equation (9) yields

Condition (g):

$$\psi_a' = \psi_l' = 0$$

Solving equation (6) for dV/dx gives

Condition (h):

$$V_a' = m_a\omega^2\zeta_a$$

Condition (i):

$$V_l' = m_l\omega^2\zeta_l$$

These conditions may now be expressed in matrix form. For the lower boundary conditions it follows that

$$\begin{Bmatrix} \zeta_a' \\ \zeta_a \\ \psi_a' \\ \psi_a \\ V_a' \\ V_a \\ M_a' \\ M_a \end{Bmatrix} = \begin{Bmatrix} \psi_a \\ \zeta_a \\ 0 \\ \psi_a \\ m_a\omega^2\zeta_a \\ 0 \\ -Z_a\omega^2\psi_a \\ 0 \end{Bmatrix} = \begin{bmatrix} 1 & 0 \\ 0 & 1 \\ 0 & 0 \\ 1 & 0 \\ 0 & m_a\omega^2 \\ 0 & 0 \\ -Z_a\omega^2 & 0 \\ 0 & 0 \end{bmatrix} \begin{Bmatrix} \psi_a \\ \zeta_a \end{Bmatrix} \tag{34}$$

and for the upper boundary conditions

$$\begin{Bmatrix} \zeta_l' \\ \zeta_l \\ \psi_l' \\ \psi_l \\ V_l' \\ V_l \\ M_l' \\ M_l \end{Bmatrix} = \begin{Bmatrix} \psi_l \\ \zeta_l \\ 0 \\ \psi_l \\ m_l\omega^2\zeta_l \\ 0 \\ -Z_l\omega^2\psi_l \\ 0 \end{Bmatrix} = \begin{bmatrix} 1 & 0 \\ 0 & 1 \\ 0 & 0 \\ 1 & 0 \\ 0 & m_l\omega^2 \\ 0 & 0 \\ -Z_l\omega^2 & 0 \\ 0 & 0 \end{bmatrix} \begin{Bmatrix} \psi_l \\ \zeta_l \end{Bmatrix} \tag{35}$$

Calculation of Frequencies

Suppose now that a number of stations have been established at definite points x_n along the span of the beam. The system variables at all stations are then uniquely determined if values are assigned to ζ_a, ψ_a, and ω.

Equation (34) determines the system variables at $x = x_a$. Equation (27) yields the system variables at $x = x_n$ in terms of the values at $x = x_a$. Once the variables at $x = x_a$ are known, equation (27) may be used again to compute the variables at $x = x_{a+1}$, and this process may be continued until the system variables at all stations are known. This process will be termed "a solution of the system" for the given values of ζ_a, ψ_a, and ω. The principle of superposition of solutions is employed by using an arbitrary value of ω in two separate solutions. The first solution has $\zeta_a = 1$, $\psi_a = 0$ and is called the "A" solution; the second has $\zeta_a = 0$, $\psi_a = 1$ and is called the "B" solution. Then by using conditions (a) and (g) of the section on boundary conditions, it can be concluded that

$$\begin{Bmatrix} \psi'_l \\ V_l \end{Bmatrix} = \begin{bmatrix} \psi'_{lA} & \psi'_{lB} \\ V_{lA} & V_{lB} \end{bmatrix} \begin{Bmatrix} \psi_a \\ \zeta_a \end{Bmatrix} = \begin{bmatrix} A_1 & B_1 \\ A_2 & B_2 \end{bmatrix} \begin{Bmatrix} \psi_a \\ \zeta_a \end{Bmatrix} = 0 \tag{36}$$

The subscripts A and B designate the separate solutions for the aforementioned boundary constraints. The coefficients A_1, A_2, B_1, and B_2 are essentially influence coefficients where A_1 and A_2 are the values of ψ' and V, respectively, at x_l due to a unit value of ψ at x_a. The values of ψ' and V, respectively, at x_l due to a unit value of ζ at x_a are termed B_1 and B_2.

Nontrivial solutions of equation (36) exist if, and only if, the determinant of the square matrix is zero. The natural frequencies are therefore determined by the equation

$$\begin{vmatrix} A_1 & B_1 \\ A_2 & B_2 \end{vmatrix} = 0 \tag{37}$$

hereinafter referred to as the frequency equation $f(\omega)$. The coefficients of equation (37) are frequency dependent as is evident from inspection of the P_{n+1} matrix defined by equations (30), (32), and (33). This frequency dependency permits the satisfaction of equation (37) and yields the natural frequencies of the system. Also, from superposition of the "A" and "B" solutions, the following additional relationships can be stated:

$$\begin{Bmatrix} \zeta_l \\ \psi_l \end{Bmatrix} = \begin{bmatrix} \zeta_{lA} & \zeta_{lB} \\ \psi_{lA} & \psi_{lB} \end{bmatrix} \begin{Bmatrix} \psi_a \\ \zeta_a \end{Bmatrix} = \begin{bmatrix} C_1 & D_1 \\ C_2 & D_2 \end{bmatrix} \begin{Bmatrix} \psi_a \\ \zeta_a \end{Bmatrix} \tag{38}$$

where C_1, C_2, D_1, and D_2 are influence coefficients for ζ_l and ψ_l.

From the second row of equation (36)

$$A_2\psi_a + B_2\zeta_a = 0 \tag{39}$$

Hence,

$$\psi_a = -\frac{B_2\zeta_a}{A_2} \tag{40}$$

From the first row of equation (38)

$$\zeta_l = C_1\psi_a + D_1\zeta_a \tag{41}$$

Solving equation (41) for ζ_a and substituting equation (40) for ψ_a gives

$$\zeta_a = \frac{A_2\zeta_l}{A_2D_1 - B_2C_1}$$

and normalizing in terms of $\zeta_l = 1$ yields

$$\zeta_a = \frac{A_2}{A_2D_1 - B_2C_1} \tag{42}$$

Substituting equation (42) in equation (40) yields

$$\psi_a = \frac{-B_2}{A_2D_1 - B_2C_1} \tag{43}$$

It is reminded that the appropriate values of A_1, A_2, B_1, B_2, C_1, C_2, D_1, and D_2 are only those associated with "A" and "B" solutions satisfying equation (37). The numerical procedure in obtaining valid solutions

is to perform trial solutions for assumed values of ω until equation (37) is satisfied. The lowest frequency satisfying the equation yields the fundamental natural mode of vibration. Succeeding higher frequencies, which satisfy equation (37), yield the progression of overtones or higher modes.

Mode Shapes and Related Data

The coefficients A_1 to D_2 associated with the proper values of ω which satisfy equation (37), when substituted into equations (42) and (43), yield appropriate initial values of ζ_a and ψ_a for the mode shapes. The recurrence formula of equation (27) relates the modal characteristics at a given station to an adjacent station. Thus, having the initial values leads to a complete solution for all stations. Such a solution yields the mode shapes, cross-section rotations, mode moments, mode shears, and the first derivatives with respect to x of each function.

It should be noted that in letting ζ_l equal unity in obtaining equations (42) and (43), the system variables derived from use of the two relationships are henceforth compatible with the mode shape normalized at $x = x_l$ (i.e., $\zeta_l = 1$). For purposes of preventing conflicts in units, it should be understood, that the form of the system variables, when $\zeta_l = 1$, is in essence

$$\left\{ X \right\} = \left\{ \frac{X}{\zeta_l} \right\} \tag{44}$$

That is, ζ, ψ, V, and M from a final solution are actually the ratios ζ_n/ζ_l, ψ_n/ζ_l, V_n/ζ_l, and M_n/ζ_l, respectively. These ratios are the system variables per unit of mode deflection at $x = x_l$.

Treatment of Discontinuities

In most practical problems associated with nonuniform beams, EI, KAG, Z, and m exhibit many discontinuities over the range $x_a \leqq x \leqq x_l$. Consequently, provisions must be made for a convenient solution across discontinuities. When a discontinuity is crossed, the system variables have to be reevaluated.

From physical consideration ψ, ζ, M, and V are continuous, and it will be shown that ψ', ζ', M', and V' are discontinuous.

Let the subscripts (-) and (+) denote values of system variables at a discontinuity which is approached through values of x lower than or higher than, respectively, the value of x at the discontinuity.

Then from equation (9) where $M_{(-)} = M_{(+)}$

$$\frac{d\psi_{(+)}}{dx} = \frac{M_{(-)}}{EI_{(+)}} \tag{45}$$

From equation (8) where $V_{(-)} = V_{(+)}$ and $\psi_{(-)} = \psi_{(+)}$

$$\frac{d\zeta_{(+)}}{dx} = \psi_{(-)} - \frac{V_{(-)}}{KAG_{(+)}} \tag{46}$$

and from equation (7)

$$\frac{dM_{(+)}}{dx} = V_{(-)} - Z_{(+)}\omega^2\psi_{(-)} \tag{47}$$

From equation (6) with $\zeta_{(-)} = \zeta_{(+)}$

$$\frac{dV_{(+)}}{dx} = m_{(+)}\omega^2\zeta_{(-)} \tag{48}$$

The relationship across a discontinuity may then be shown in matrix form

$$\left\{X_{(+)}\right\} = \begin{bmatrix} 0 & 0 & 0 & 1 & 0 & -\frac{1}{KAG_{(+)}} & 0 & 0 \\ 0 & 1 & 0 & 0 & 0 & 0 & 0 & 0 \\ 0 & 0 & 0 & 0 & 0 & 0 & 0 & \frac{1}{EI_{(+)}} \\ 0 & 0 & 0 & 1 & 0 & 0 & 0 & 0 \\ 0 & m_{(+)}\omega^2 & 0 & 0 & 0 & 0 & 0 & 0 \\ 0 & 0 & 0 & 0 & 0 & 1 & 0 & 0 \\ 0 & 0 & 0 & -Z_{(+)}\omega^2 & 0 & 1 & 0 & 0 \\ 0 & 0 & 0 & 0 & 0 & 0 & 0 & 1 \end{bmatrix} \left\{X_{(-)}\right\} \tag{49}$$

This relationship is exactly satisfied when $\Delta x = 0$ is entered into P_{n+1} of equation (33). This contributes to the efficiency of the method for use in conjunction with high-speed digital computers because the same recurrence formulas are used to relate system variables across a discontinuity as are used to relate variables across a finite interval.

Orthogonality Condition

One of the major uses of natural mode data is in modal form series solutions. Their practical applications in series solutions is a result of the many simplifications that result from their orthogonality relationships. These relationships for modal solutions, restricted to elementary beam theory, are well known and widely referenced in reports and standard texts on elementary vibrations. The addition of rotary inertia and shear deformation alters the conventional relationship and a clear description of the orthogonality relationship for nonuniform free-free beams with secondary effects is considered essential to the completeness of this paper. In reference 6, Leonard derives the orthogonality relationships for the uniform free-free beam with shear deformation and rotary inertia. In the following discussion, the conditions for the nonuniform free-free beam will be set forth.

Substituting equation (8) into equation (6) and adding subscripts to ζ and ψ to designate the specific mode r yields

$$m\omega_r^2\zeta_r + \frac{d}{dx}\left[KAG\left(\frac{d\zeta_r}{dx} - \psi_r\right)\right] = 0 \tag{50}$$

Also, substituting equations (8) and (9) in equation (7) gives

$$KAG\left(\psi_r - \frac{d\zeta_r}{dx}\right) - Z\omega_r^2\psi_r - \frac{d}{dx}\left(EI\,\frac{d\psi_r}{dx}\right) = 0 \tag{51}$$

Multiplying equation (50) by ζ_n and (51) by ψ_n, adding both results together, and integrating over the length of the beam, yields

$$\begin{aligned}\omega_r^2\int_{x_a}^{x_l}\left(m\zeta_n\zeta_r + Z\psi_n\psi_r\right)dx = &-\int_{x_a}^{x_l}\zeta_n\frac{d}{dx}\left[KAG\left(\frac{d\zeta_r}{dx} - \psi_r\right)\right]dx \\ &- \int_{x_a}^{x_l}\psi_n\frac{d}{dx}\left(EI\,\frac{d\psi_r}{dx}\right)dx \\ &- \int_{x_a}^{x_l}KAG\left(\psi_n\frac{d\zeta_r}{dx} - \psi_r\psi_n\right)dx\end{aligned} \tag{52}$$

Since the r and n subscripts have been selected arbitrarily, equation (52) is equally valid when expressed by reversing r and n. Making this reversal yields

$$\omega_n^2 \int_{x_a}^{x_l} \left(m\zeta_n\zeta_r + Z\psi_n\psi_r \right) dx = -\int_{x_a}^{x_l} \zeta_r \frac{d}{dx}\left[KAG\left(\frac{d\zeta_n}{dx} - \psi_n \right) \right] dx$$

$$- \int_{x_a}^{x_l} \psi_r \frac{d}{dx}\left(EI \frac{d\psi_n}{dx} \right) dx$$

$$- \int_{x_a}^{x_l} KAG\left(\psi_r \frac{d\zeta_n}{dx} - \psi_n\psi_r \right) dx \qquad (53)$$

Expanding equations (52) and (53) by integrating, by parts, the first and second terms on the right-hand side of the equations and then subtracting the extended version of (53) from the extended form of (52) will yield

$$\left(\omega_r^2 - \omega_n^2 \right) \int_{x_a}^{x_l} \left(m\zeta_n\zeta_r + Z\psi_n\psi_r \right) dx = -\zeta_n KAG\left(\frac{d\zeta_r}{dx} - \psi_r \right)\Bigg|_{x_a}^{x_l} + \zeta_r KAG\left(\frac{d\zeta_n}{dx} - \psi_n \right)\Bigg|_{x_a}^{x_l}$$

$$- \psi_n EI \frac{d\psi_r}{dx}\Bigg|_{x_a}^{x_l} + \psi_r EI \frac{d\psi_n}{dx}\Bigg|_{x_a}^{x_l} \qquad (54)$$

For the free-free boundary conditions

$$\left.\begin{aligned} KAG\left(\frac{d\zeta_n}{dx} - \psi_n \right)\Bigg|_{x_a}^{x_l} &= V_n(x_a) - V_n(x_l) = 0 \\ EI \frac{d\psi_n}{dx}\Bigg|_{x_a}^{x_l} &= M_n(x_l) - M_n(x_a) = 0 \end{aligned}\right\} \text{Equally valid for n or r} \qquad (55)$$

With these relationships, equation (54) leads to the final conclusion that

$$\left(\omega_r^2 - \omega_n^2 \right) \int_{x_a}^{x_l} \left(m\zeta_n\zeta_r + Z\psi_n\psi_r \right) dx = 0 \qquad (56)$$

and when $\omega_n \neq \omega_r$, it is necessary that

$$\int_{x_a}^{x_l} \left(m\zeta_n\zeta_r + Z\psi_n\psi_r \right) dx = 0 \qquad \omega_n \neq \omega_r \qquad (57)$$

When $\omega_n = \omega_r$, it is usual to define the preceding integral as the effective mass of the mode.

$$m_r = \int_{x_a}^{x_l} \left(m\zeta_r^2 + Z\psi_r^2 \right) dx \qquad \omega_n = \omega_r \qquad (58)$$

To avoid confusion and to obtain the effective mass in terms of mass units (lb-sec^2/in.), it is necessary only to interpret the symbols ζ_r and ψ_r as applicable to the dimensionless mode.

Now, instead of subtracting as was done to obtain equation (54), the equations are added; then with the additional results of equation (57) when $n \neq r$, it is found that

$$\int_{x_a}^{x_l} \left[EI \frac{d\psi_r}{dx} \frac{d\psi_n}{dx} + KAG\left(\frac{d\zeta_n}{dx} - \psi_n \right)\left(\frac{d\zeta_r}{dx} - \psi_r \right) \right] dx = 0 \qquad n \neq r \qquad (59)$$

and when $n = r$, it is usual to define the preceding integral as the effective spring constant of the mode:

$$k_r = \omega_r^2 m_r = \int_{x_a}^{x_l} \left[EI \frac{d\psi_r^2}{dx} + KAG\left(\frac{d\zeta_r}{dx} - \psi_r \right)^2 \right] dx \qquad n = r \qquad (60)$$

where the same statement regarding units for equation (58) applies.

Equations (57) and (59) are the orthogonality properties of the free-free beam of variable mass and stiffness with shear deformation and rotary inertia.

Equations (58) and (60) are useful relationships defining the effective mass and effective spring of the rth mode referenced at the normalizing point of the mode shape $\zeta_r = 1$.

Equilibrium Relationships

In addition to the useful orthogonality relationships, two other valuable integrals associated with the equilibrium of the mode are frequently encountered. For the free-free system to possess dynamic equilibrium while undergoing natural vibrations, the following relationships prevail:

$$\int_{x_a}^{x_l} m\zeta_r \, dx = 0 \tag{61}$$

$$\int_{x_a}^{x_l} \left(m\zeta_r x + Z\psi_r \right) dx = 0 \tag{62}$$

SOME ASPECTS OF APPLICATIONS

Basic relationships for the recurrence solution of the beam vibration problem are given in equations (27), (30), (32), and (33). The natural frequencies are obtainable from equation (37). Orthogonality and equilibrium relationships are given in equations (57), (59), (61), and (62).

Descriptiveness of Output Data

The type of solution set forth by the foregoing equations is inherently adaptable to producing highly descriptive modal data. It has been shown by equation (49) that ψ', ζ', M', and V' are discontinuous functions by virtue of discontinuities in EI, KAG, Z, and m. The quantities obtained by the solution are of equal descriptiveness to that of the input data; that is, for every discontinuity in input data (EI, KAG, Z, and m) there will result an associated discontinuity in the output functions. The quality of these data cannot be equaled by the discrete mass methods of analysis such as that of reference 3. The method is also inherently suitable for automatic digital-plotting routines since the input can be supplied or generated by interpolation to a definition as fine as desired to give an acceptable plot of output.

Numerical Solutions

The successful use of the foregoing formulation is largely dependent on the details of the computer program. Several important features to be observed are set forth in the following text.

Machine time.- Improper programing can result in lengthy computing times yielding unreasonably costly data. Conversely, proper programing for minimum computer time can be most rewarding with the subject formulation. For example,

programing the inverted and extended form of equation (28) given by equations (32) and (33) reduced the machine time to one-fourth that required by a program performing internally the operations of equation (28). Unduly stringent accuracy requirements in determining the natural frequencies by equation (37) can also result in exorbitant machine time. Extensive use of the method of this paper has indicated that three modes with frequency convergence to 0.1 percent error can be achieved with around 300 stations of input data to an IBM 7094 electronic data processing system in about 5 minutes. It should be noted that this accuracy on frequency is valid for the mathematical model but it is not indicative of the accuracy of predicting the frequencies of the actual structure. The accuracy is obviously dependent on the appropriateness of the math model.

Attempting to satisfy upper boundary conditions to unneccessary accuracies can also be costly. For example, ψ'_l, V_l, and M_l are zero for the free-free boundary case. These absolute conditions cannot be achieved by digital computers. The analyst, however, should accept finite boundary values that are a fraction of 1 percent of the peak absolute values of their respective functions over the total span $x_a \leqq x \leqq x_l$. Boundary values which are zero correct to the fifth significant figure of the maximum value of a function can readily be obtained.

Near zero stiffness.- In applying the recurrence technique of this report the unwary analyst can be confused and misled by using inputs of KAG and EI that are near zero at or near the upper boundary position. This condition is encountered particularly with pointed nose cones or other similar structures that essentially taper to zero. The problem manifests itself in a radical variation of the mode shape in the area approaching the upper boundary of the span. This variation is a combined result of near zero stiffness of KAG and/or EI and the failure to achieve numerically the absolute theoretical zero boundary condition. This condition is readily corrected by avoiding, near the free ends, KAG and EI input values of less than 0.0001 of their respective average values over the total span.

Superposition for final modes.- The sequential nature of a solution by the method proposed in this paper is as follows: First, obtain for a variety of frequencies the influence coefficients A_1, A_2, B_1, and B_2 by the "A" and "B" solutions discussed in "Calculation of Frequencies." From this trial technique, a frequency is discerned to a desirable accuracy that will satisfy the frequency equation (eq. (37)). Second, after obtaining a natural frequency, the influence coefficients associated with the critical frequency are substituted into equations (42) and (43) to obtain the boundary values ζ_a and ψ_a associated with the normalized natural mode. Finally, with the knowledge of ω, ζ_a, and ψ_a, all initial conditions and coefficients can be fully ascertained, and the recurrence solution of equation (27) can be extended over the total span. This solution yields data on all of the system variables for all desired stations. An important feature associated with this last operation should be noted. Entering ζ_a and ψ_a simultaneously into equation (27) in the final solution for the modal characteristics is a different digital operation than the original procedure of superposition that led to knowledge of ζ_a

and ψ_a. Consequently, a simultaneous solution will result in different digital round-off errors that will reduce the accuracy of the final boundary values below that previously established by superposition. Since a large number of significant figures are essential to the mechanism of the numerical solution, a duplicate procedure for the initial operation is recommended in obtaining the final modal data. The available values of ζ_a and ψ_a should be used in independent "A" and "B" solutions and should be combined at corresponding x stations to obtain the desired final modal data.

Integration intervals.- The fundamental differential equations of motion given by equation (10) are all of first order. Integration is performed on all variables with the assumption of linear variations of the first derivatives as defined by equations (12) to (15). For this assumption to be acceptable, the Δx interval must at all stations be suitably small. Studies on interval sizes have shown that adequate results are normally obtainable by describing the physical characteristics of a vehicle at all points of discontinuity with the added constraint that $\Delta x = L/100$. The latter constraint is easily programed into the computer and obviates a large amount of repetitive input data over long constant sections. In addition, where continuous but nevertheless radical variations occur in the input functions, additional stations should be included to insure that the variations are adequately defined.

Frequency search technique.- The economy of the machine solution is intimately associated with the iterative technique employed to obtain the unique frequencies that will satisfy equation (37). Equation (37) is of the form

$$f(\omega) = 0$$

and must be solved by trial and error.

Successful results have been achieved by performing repeated trial solutions for $f(\omega)$ by systematically increasing the frequency ω by $\Delta\omega$ until a sign change is indicated, i.e.,

$$\frac{f\left(\omega^{n+1}\right)}{f\left(\omega^{n}\right)} < 0$$

where ω^n is the nth trial value. At this point, a second-order (parabolic) curve fit is applied to points at $f\left(\omega^{n-1}\right)$, $f\left(\omega^{n}\right)$, and $f\left(\omega^{n+1}\right)$ and the resulting analytical expression can be solved for ω where $f(\omega) = 0$. This operation can be continued with each improved frequency until the difference between successive frequencies is less than some preassigned tolerance.

Convergence can be hurried by good estimates of $\Delta\omega$ for the specific problem and refraining from a too stringent tolerance in frequency. Increasing $\Delta\omega$ and the frequency tolerance for successive overtones is also advantageous in maintaining machine time within practical limits.

Secondary Influences

A principal objective of the mathematical development of this paper was to provide a means for including, as well as investigating, the effects of the secondary contributions of shear deformation and rotary inertia in modal analyses.

Comparison with classical cases.- Studies have been made by comparing the classical or exact modal data for uniform free-free beams without secondary effects with data obtained by the subject recurrence technique with secondary effects. The two methods, secondary effects being excluded, agreed to an accuracy of greater than 0.01 percent on the first three mode frequencies, mode shapes, and nodal points. It was felt that this agreement qualified the numerical technique for use in further comparative studies.

The salient results of some studies to determine the significance of shear and rotary inertia on the classic uniform beam are furnished in figure 1. Data were derived for a solid cylindrical beam and for a thin-wall cylindrical beam of a thickness-to-diameter ratio of 0.015. Since the effectiveness of shear deformation is dependent upon the ratio of the shear modulus G to the bending modulus E, the studies were made for both fiber-glass and steel beams. It can be seen from the curves for the steel beam, that for either of the cross sections the combined secondary influences caused frequency reductions in the first three modes of not greater than 5 percent when ratios of length to diameter (L/D) are greater than 20. This frequency reduction compares with those reductions of up to 14 percent for values of L/D greater than 20 for fiber-glass beams. The value of G/E for the fiber-glass beam was 0.20 whereas that for the steel beam was 0.42. It is also evident that the frequency reductions for both the steel and fiber-glass beams are more pronounced for the thin-wall cases than for the solid beams. As the aspect ratio (L/D) decreases, the reduction in frequency becomes quite pronounced and reaches more than 50 percent in the third mode for the thin-wall cases for aspect ratios of 4 and 7 for the steel and fiber-glass beams, respectively.

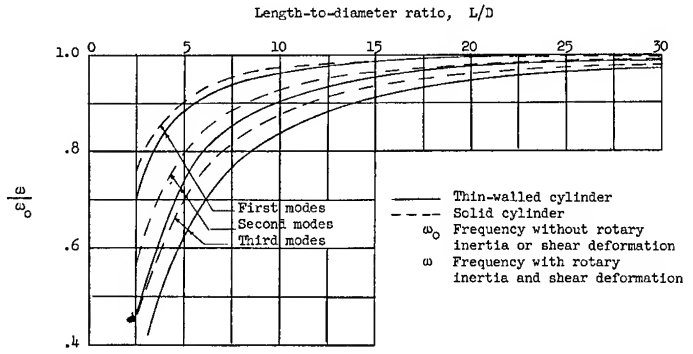

(a) Steel beam.

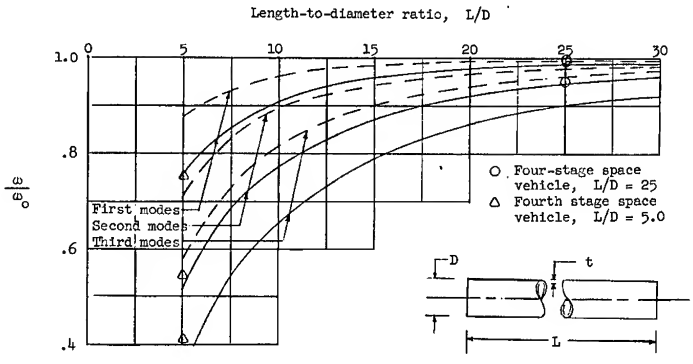

(b) Fiber-glass beam.

Figure 1.- Effects of rotary inertia and shear deformation on the frequencies of free-free vibrations of uniform cylindrical beams.

In reference 7, Kruszewski presented closed-form solutions for the uniform beam with shear deformation and rotary inertia. The report gives general data for readily determining the significances of the secondary influences for general beam cross section and elastic properties. The curves of figure 1 obtained by the numerical procedure of this paper were checked against the data from the closed-form solution of reference 7 and were found to be in nearly perfect agreement. This comparison further qualifies the numerical technique as a satisfactory and accurate procedure for incorporating the secondary influences into the beam solution.

Effects on launch vehicle.- The six data points given in the fiber-glass curves of figure 1 show the frequency reductions due to secondary influences on a four-stage space vehicle with $L/D = 25$ and the fourth stage of a space vehicle with $L/D = 5$. Of the first-stage length 3.5 percent was fiber glass and 26 percent of the fourth-stage length was fiber glass. The first-stage data reveal reductions greater than those predicted for thin-wall steel beams but are less, as would be expected, than those for thin-wall fiber-glass beams.

The fourth-stage frequencies for $L/D = 5$ were significantly reduced by the secondary effects and closely correspond to the reductions predicted for the thin-wall fiber-glass beam. It appears that the fiber glass appreciably contributed to the frequency reduction even though the fiber glass extended over only one-fourth of the stage length. The fiber-glass section extended over a span running from 0.23 to 0.55 of the length which was a region subjected to a significant proportion of the shearing action. The specific vehicle for which these data were derived is documented further in the section entitled "NUMERICAL EXAMPLE."

Measure of significance.- The aforementioned considerations suggest the usefulness of the curves of figure 1 in estimating the probable significance of shear deformation and rotary inertia in free-free natural frequencies of launch vehicles. Both the vehicle data and the curves clearly indicate the necessity of including secondary influences if accurate analyses are desired on low-aspect ratio structures.

NUMERICAL EXAMPLE

An example is presented of an application of the recurrence solution to the actual research vehicle illustrated in figure 2. Solutions have been provided for the first- and fourth-stage configurations of flight. These two cases are submitted to show an actual numerical example derived from the subject method and to illustrate the varying importance of secondary effects with the vehicle's length-to-diameter ratio. The basic physical

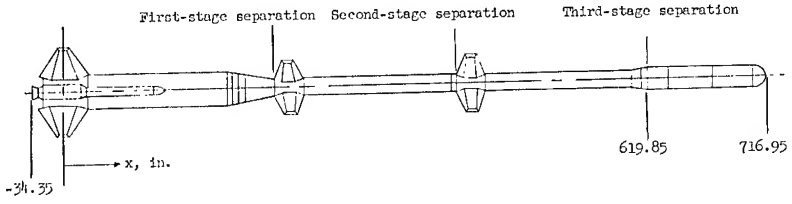

Figure 2.- Typical multistage research launch vehicle.

characteristics of the vehicle required as input to the program have been recorded and submitted in table I. The tabulation provides input for both cases by taking the physical characteristics at $x = 619.85$ as the first applicable quantities for the fourth-stage analysis.

Frequency Data

In table II, the frequencies and percent reduction in frequencies are given for the first three modes of vibration for the two stages of the vehicle of figure 2. The data are displayed for analyses without the secondary effects, with both effects, with rotary inertia only, and with shear deformation only.

Inspection of the data for the first stage will show only small effects of shear deformation and rotary inertia. The influences grow progressively with increasing modes as would be normally anticipated. The maximum contribution of rotary inertia and shear deformation is seen to be a reduction in frequency of slightly less than 5 percent on the third mode. The first-stage configuration has a length-to-diameter ratio of approximately 25. In the fourth-stage configuration with an aspect ratio of 5.0, the importance of rotary inertia and shear deformation are quite evident. The combined secondary influences produce a reduction of 58 percent in values computed without consideration of shear deformation and rotary inertia. The significance also increases with increasing modes. These results strongly suggest that for reliable frequency calculations on the upper stages of typical launch vehicles, consideration of the secondary contributions to flexure must be given.

It is interesting to note, however, that good results would have been obtained in all cases shown by incorporating in the solution the effects of shear deformation only. The frequency error most affected by the secondary influence (third mode of the fourth stage) would be slightly less than 7 percent if shear deformation only had been considered.

Elastic Curve Characteristics

A graphical comparison of the modal functions for the first three natural modes for the first stage of the example vehicle would reveal only trivial departure from concurrency. However, it will be shown later that this is not the case for the fourth-stage configuration where the secondary effects have been shown to be appreciable.

Mode shapes.- In figure 3, the fourth-stage mode shapes ζ are compared for solutions with and without secondary effects. The comparison of mode shapes was accomplished by the application of the method of least squares. In spite of the severe reductions noted in frequencies, the first three mode shapes retain similar graphical characteristics.

Mode shape inflections near tips.- An interesting elastic curve characteristic should be noted that results from the inclusion of shear deformation. For beams with secondary effects, an inflection in the mode shape is frequently observed near one or both of the free ends and outboard of the outermost nodal

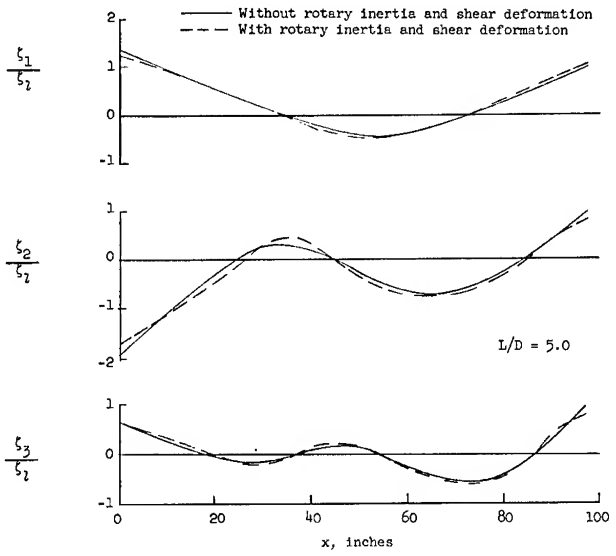

Figure 3.- Effects of rotary inertia and shear deformation on mode shapes of a low-aspect-ratio upper stage of a launch vehicle.

point. Inspection of either of the three modes of figure 3 will indicate the inflection or reversal in curvature on the right-hand end in the vicinity of $x = 90$ inches. The inflection point occurs when the second derivative of the mode shape becomes zero. An expression is readily obtained by differentiating equation (8) that indicates the parameters involved in the phenomenon, that is

$$\frac{d^2\zeta}{dx^2} + \frac{d}{dx}\left(\frac{V}{KAG}\right) - \frac{d\psi}{dx} = 0 \qquad (63)$$

since

$$\frac{d^2\zeta}{dx^2} = 0$$

at the inflection point, and

$$\frac{d^2\zeta}{dx^2} < 0$$

to the right of the inflection point. Then it follows from equation (63) that for the dip in the elastic curve on the end to occur

$$\frac{d}{dx}\frac{V}{KAG} \geqq \frac{d\psi}{dx} \qquad (64)$$

Equation (64) simply states that when curvature contribution due to shear deformation is greater than the curvature contribution to the elastic curve due to bending, the inflection near the tip will be evident. In elementary beam solutions, shear deformation is not considered; this case corresponds to the limiting case where $KAG \to \infty$. It is then obvious from equation (64) that for cases where shear deformation is ignored, the shear deformation contribution to curvature is zero and the conditions of equation (64) can never be realized.

Mode slopes.- A pronounced departure between data computed with and without secondary effects is seen in the comparison of mode slopes in figure 4. The solid curves are the slopes computed without shear deformation and rotary inertia. The dashed curves were computed with secondary effects. The slopes are compatible with the amplitudes of the mode shapes given in figure 3 as established by the least-squares method. The most conspicuous differences are the discontinuities that are evident in the data incorporating rotary inertia and shear deformation. The discontinuities result from shear deformation and are not evident in results without shear deformation, whether including rotary inertia or not. Accurate mode slopes frequently are required in system

stability studies of autopilot structural feedback. It is evident from figure 4 that, for accurate structural feedback analyses on short L/D configurations, the secondary effects, particularly shear deformation, should be included in developing the required mode slopes.

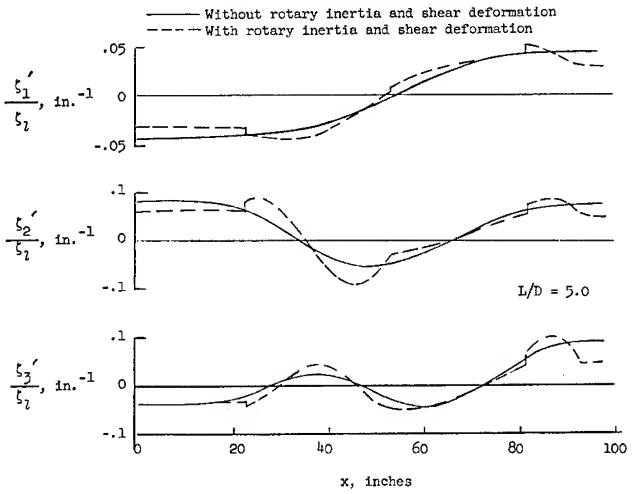

Figure 4.- Effects of rotary inertia and shear deformation on mode slopes of a low-aspect-ratio upper stage of a launch vehicle.

Mode slopes compared with cross-section rotation.- In elementary beam theory, which ignores both rotary inertia and shear deformation, the cross-section rotation is quantitatively the same as the slope. The differences between the slope of the elastic curve ζ' and the cross-section rotation ψ are a further measure of the significance of secondary effects. A comparison of these modal functions is shown graphically in figure 5 for the fourth stage of the example vehicle. The observed differences between ζ' and ψ are completely a result of shear deformation and are not evident in solutions ignoring shear.

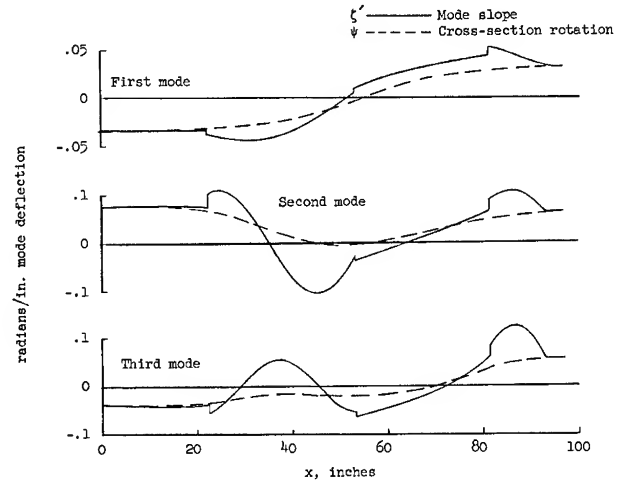

Figure 5.- Comparison of cross-section rotations and mode slopes of a low-aspect-ratio upper stage of a launch vehicle. (All curves include the effects of shear and rotary inertia.)

Load Characteristics of Modes

The moment and shear distributions for the fourth stage of the example vehicle of figure 2 are submitted in figures 6 and 7. Comparative curves are given for data calculated with and without the secondary influences of shear deformation and rotary inertia. The moment and shear values are compatible with the relative mode amplitudes shown in figure 3 and as established by the least-squares method of comparison. Both the moment and shear data show significant differences with increasing modes between solutions with and without secondary influences, the magnitudes of the differences increasing with increasing modes. An appreciable separation in the right nodal point of the third mode moment curves is observed. The startling differences that are observed between amplitudes of the comparative data for the second and third

modes are principally attributed to the lower frequencies and consequently lower inertia loading on the beam for the solutions with secondary effects.

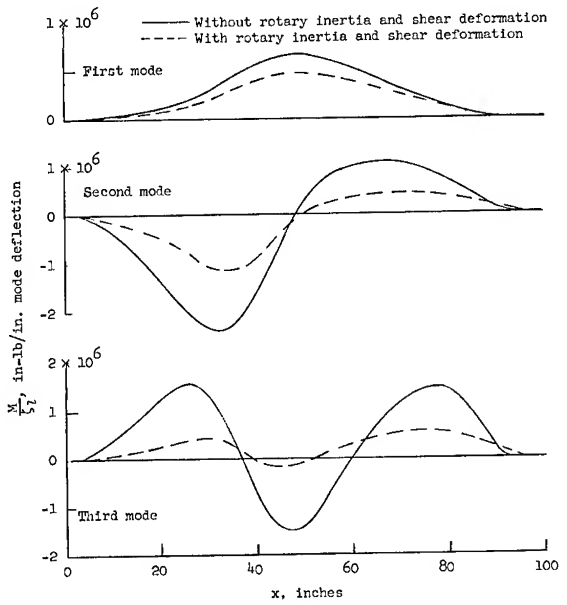

Figure 6.- Comparison of the mode moments from solutions with and without secondary effects for a low-aspect-ratio upper stage of a launch vehicle.

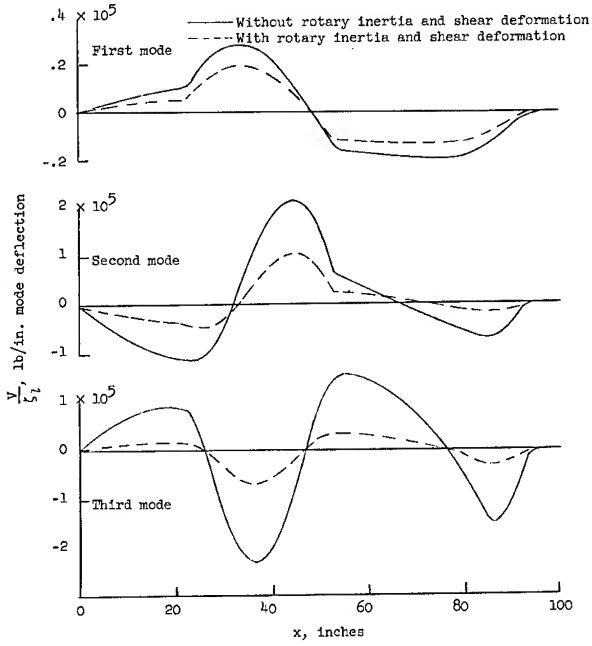

Figure 7.- Comparison of mode shears from solutions with and without secondary effects for a low-aspect-ratio upper stage of a launch vehicle.

CONCLUDING REMARKS

A recurrence solution is presented that is especially suitable for obtaining highly descriptive modal data on severely discontinuous nonuniform beamlike structures; the solution includes the secondary influences of rotary inertia and shear deformation. Data are provided for helping the analyst in estimating the probable significance of shear deformation and rotary inertia in free-free natural frequencies of launch vehicles.

Numerical examples of the solution are included for a first-stage and a fourth-stage configuration of a research vehicle. The secondary influences of rotary inertia and shear deformation had trivial effects on the first-stage data, but were found to have very significant effects on the data for the fourth stage.

In most practical applications to launch vehicles, it is concluded that shear deformation is considerably more important than rotary inertia. Acceptable results could generally be obtained by including shear deformation only.

The authors' experiences indicate that, in general, for most beam applications the secondary influences have the least obvious effect on the mode shapes. An appreciable influence is noted in reducing frequencies and large effects are experienced on the mode shears and moments. The appearance of discontinuities in the mode slopes is a further influence resulting from the consideration of shear deformation.

The addition of shear deformation to elementary beam vibration theory can result in an inflection in the mode shape outboard of the outermost nodal points.

Successful and economical solutions by the subject method are intimately dependent upon details of the computing program. Some salient points are discussed on appropriateness of input data, superposition problems, numerical integration intervals, and frequency iteration routine.

Langley Research Center,
National Aeronautics and Space Administration,
Langley Station, Hampton, Va., April 9, 1965.

REFERENCES

1. Den Hartog, J. P.: Mechanical Vibrations. Third ed., McGraw-Hill Book Co. Inc., 1947, pp. 185-205.

2. Scanlan, Robert H.; and Rosenbaum, Robert: Introduction to the Study of Aircraft Vibration and Flutter. The Macmillan Co., 1951, pp. 177-180.

3. Alley, Vernon L., Jr.; and Gerringer, A. Harper: A Matrix Method for the Determination of the Natural Vibrations of Free-Free Unsymmetrical Beams With Application to Launch Vehicles. NASA TN D-1247, 1962.

4. Houbolt, John C.; and Anderson, Roger A.: Calculation of Uncoupled Modes and Frequencies in Bending or Torsion of Nonuniform Beams. NACA TN 1522, 1948.

5. Spector, Joseph: Integral Series Solution for Uncoupled Vibrations of Nonuniform Bars. Master Appl. Mech. Thesis, Univ. of Virginia, 1952.

6. Leonard, Robert W.: On Solutions for the Transient Response of Beams. NASA TR R-21, 1959. (Supersedes NACA TN 4244.)

7. Kruszewski, Edwin T.: Effect of Transverse Shear and Rotary Inertia on the Natural Frequency of a Uniform Beam. NACA TN 1909, 1949.

TABLE I.- PHYSICAL CHARACTERISTICS OF A MULTISTAGE LAUNCH VEHICLE

x, in.	Z, lb-sec^2	m, lb-sec^2/in.^{2}	EI, lb-in.^{2}	KAG, lb
-34.35	1.70	0.01743	0.100×10^9	10.00×10^6
-19.35	1.70	.01743	.100	10.00
-19.35	14.70	.06030	14.770	33.54
0	14.70	.06030	14.770	33.54
17.85	14.70	.06030	6.743	33.54
17.85	14.70	.06030	6.743	33.54
19.35	14.70	.06030	6.743	33.54
19.35	13.59	.13094	6.743	59.34
20.85	13.59	.13094	6.743	59.34
20.85	13.59	.13094	34.59	59.34
71.65	13.59	.13094	34.59	59.34
71.65	6.61	.11350	34.59	59.34
204.85	6.61	.11350	34.59	59.34
204.85	6.61	.11350	8.352	59.34
206.35	6.61	.11350	8.352	59.34
206.35	1.50	.00895	8.352	209.00
207.85	1.50	.00895	8.352	209.00
207.85	1.50	.00895	94.92	209.00
209.95	1.50	.00895	94.92	209.00
209.95	1.50	.00895	6.914	209.00
211.45	1.50	.00895	6.914	209.00
211.45	.35	.00895	6.914	26.46
212.95	.34	.00895	6.914	26.00
212.95	.34	.00895	13.900	26.00
217.95	.31	.00895	10.400	21.00
222.95	.20	.00895	8.000	17.00
227.95	.12	.00895	6.000	14.80
232.95	.05	.00895	3.200	13.60
236.35	.047	.00895	2.100	13.10
236.35	.047	.00895	1.403	13.10
237.85	.045	.00895	1.403	12.92
237.85	1.40	.01474	1.403	31.85
239.35	1.395	.01474	1.403	36.89
239.35	1.395	.01474	4.000	36.89
245.25	1.336	.01474	3.370	56.71
245.25	1.336	.01474	1.042	56.71
246.75	1.321	.01474	1.042	61.75
246.75	1.321	.01474	1.042	61.75
248.25	1.316	.01474	1.042	61.75
248.25	1.316	.01474	3.361	61.75
257.85	1.200	.01474	3.361	61.75
257.85	1.200	.03673	3.361	61.75
258.75	1.200	.03673	3.361	61.75
258.75	1.200	.03673	4.910	33.69
262.85	1.200	.03673	4.910	33.69
262.85	.385	.026668	4.910	33.69
424.85	.385	.026668	4.910	33.69
424.85	.385	.026668	1.665	33.69
426.35	.385	.026668	1.665	33.69
426.35	1.090	.011718	1.665	24.88
427.85	1.090	.011718	1.665	24.88

TABLE I.- PHYSICAL CHARACTERISTICS OF A MULTISTAGE LAUNCH VEHICLE - Concluded

x, in.	Z, lb-sec^2	m, lb-sec^2/in.^{2}	EI, lb-in.^{2}	KAG, lb
427.85	1.090	0.011718	3.025×10^9	24.88×10^6
444.85	1.090	.011718	3.025	24.88
444.85	1.090	.011718	1.071	24.88
446.35	1.090	.011718	1.071	24.88
446.35	.385	.03360	1.071	33.69
447.85	.385	.03360	1.071	33.69
447.85	.385	.03360	4.910	33.69
451.35	.385	.03360	4.910	33.69
451.35	.385	.026668	4.910	33.69
604.55	.385	.026668	4.910	33.69
604.55	.385	.026668	.5224	33.69
606.05	.385	.026668	.5224	33.69
606.05	.084	.00585	.5224	24.08
607.55	.091	.00585	.5224	24.61
607.55	.091	.00585	3.630	24.61
610.00	.103	.00585	4.080	25.48
614.00	.122	.00585	4.810	26.89
618.35	.143	.00585	5.600	28.43
618.35	.143	.00585	.8931	28.43
619.85	.150	.00585	.8931	28.96
619.85	.070	.00266	.8931	6.639
621.35	.070	.00266	.8931	6.639
621.35	.070	.00266	1.409	6.639
640.95	.070	.00266	1.409	6.639
640.95	.070	.00266	.2714	6.639
642.45	.070	.00266	.2714	6.639
642.45	.900	.04457	.2714	1.169
643.95	.900	.04457	.2714	1.169
643.95	.900	.04457	.3760	1.169
647.45	.900	.04457	.3760	1.169
647.45	.900	.04457	.3760	1.169
667.96	.900	.04457	.3760	1.169
667.96	.900	.04457	.3760	1.169
671.462	.900	.04457	.3760	1.169
671.462	.900	.04457	.20014	1.169
672.962	.900	.04457	.20014	1.169
672.962	.140	.00344	.20014	1.000
674.462	.140	.00344	.20014	1.000
674.462	.140	.00344	.250	1.000
698.45	.140	.00344	.250	1.000
698.45	.140	.01409	.250	1.000
699.76	.140	.01409	.250	1.000
699.76	.140	.01409	.1364	1.000
701.26	.140	.01409	.1364	1.000
701.26	.380	.01409	.1364	.500
702.76	.380	.01409	.1364	.500
702.76	.380	.01409	.250	.500
712.65	.380	.01409	.250	.500
712.65	.380	.000259	.250	.500
716.95	.380	.000259	.250	.500

TABLE II.- REDUCTION OF FREE-FREE NATURAL FREQUENCIES OF A MULTISTAGE RESEARCH VEHICLE DUE TO ROTARY INERTIA AND SHEAR DEFORMATION

Mode	Frequency, radians/sec				Reduction in frequency, percent		
	Without rotary inertia and shear deformation	With rotary inertia and shear deformation	With rotary inertia only	With shear deformation only	With rotary inertia and shear deformation	With rotary inertia only	With shear deformation only
Four-stage launch vehicle, aspect ratio ≈ 25							
1	16.120	16.017	16.054	16.083	0.64	0.41	0.23
2	47.457	46.521	47.195	46.770	1.97	.55	1.45
3	98.686	93.943	97.566	94.727	4.81	1.13	4.01
Fourth stage of multistage launch vehicle, aspect ratio ≈ 5.0							
1	438.557	334.776	400.968	348.945	23.66	8.57	20.43
2	1367.317	760.445	1104.970	803.663	44.38	19.19	41.22
3	2292.381	960.819	1655.463	1049.897	58.09	27.78	54.20

"The aeronautical and space activities of the United States shall be conducted so as to contribute . . . to the expansion of human knowledge of phenomena in the atmosphere and space. The Administration shall provide for the widest practicable and appropriate dissemination of information concerning its activities and the results thereof."

—NATIONAL AERONAUTICS AND SPACE ACT OF 1958

NASA SCIENTIFIC AND TECHNICAL PUBLICATIONS

TECHNICAL REPORTS: Scientific and technical information considered important, complete, and a lasting contribution to existing knowledge.

TECHNICAL NOTES: Information less broad in scope but nevertheless of importance as a contribution to existing knowledge.

TECHNICAL MEMORANDUMS: Information receiving limited distribution because of preliminary data, security classification, or other reasons.

CONTRACTOR REPORTS: Technical information generated in connection with a NASA contract or grant and released under NASA auspices.

TECHNICAL TRANSLATIONS: Information published in a foreign language considered to merit NASA distribution in English.

TECHNICAL REPRINTS: Information derived from NASA activities and initially published in the form of journal articles.

SPECIAL PUBLICATIONS: Information derived from or of value to NASA activities but not necessarily reporting the results of individual NASA-programmed scientific efforts. Publications include conference proceedings, monographs, data compilations, handbooks, sourcebooks, and special bibliographies.

Details on the availability of these publications may be obtained from:

SCIENTIFIC AND TECHNICAL INFORMATION DIVISION

NATIONAL AERONAUTICS AND SPACE ADMINISTRATION

Washington, D.C. 20546